Korean J. Chem. Eng., 39(1), 216-226 (2022)
DOI: 10.1007/s11814-021-0892-3

pISSN: 0256-1115
eISSN: 1975-7220

Kinetics, isothermal and mechanistic insight into the adsorption of eosin yellow and malachite green from water via tri-metallic layered double hydroxide nanosheets

Muhammad Altaf Nazir*, Tayyaba Najam, Muhammad Sohail Bashir***, Muhammad Sufyan Javed****, Muhammad Aswad Bashir*, Muhammad Imran*****, Umair Azhar******,†, Syed Shoaib Ahmad Shah*,***,†, and Aziz ur Rehman*,†**

*Institute of Chemistry, The Islamia University of Bahawalpur, Bahawalpur 63100, I. R. Pakistan
**Institute for Advanced Study, Shenzhen University, Shenzhen 518060, P. R. China
***Hefei National Laboratory for Physical Sciences at the Microscale, CAS Key Laboratory of Soft Matter Chemistry, School of Chemistry and Materials Science, University of Science and Technology of China, Hefei, Anhui 230026, P. R. China
****School of Physical Science and Technology, Lanzhou University, Lanzhou 730000, P. R. China
*****Department of Chemistry, Faculty of Science, King Khalid University, P.O. Box 9004, Abha 61413, Saudi Arabia
******Department of Polymer Engineering, National Textile University Karachi Campus, Karachi 74900, I. R. Pakistan
(*Received 27 February 2021 • Revised 27 May 2021 • Accepted 4 July 2021*)

Abstract−The use of highly efficient, environment-friendly and economically inexpensive materials for the adsorption removal of contaminants from water has always been considered as emerging task. In this study, we synthesized hybrid tri-metallic nickel cobalt layered double hydroxide (NiCoAl-LDH) porous material for the adsorption removal of Eosin yellow (EY) and Malachite green (MG) from water. The characterization results disclosed that tri-metallic LDH has been synthesized with extraordinary purity, identical morphology and high surface area (134.21 $m^2 \cdot g^{-1}$). The NiCoAl-LDH performs the best for adsorption of EY (q_e=37.30 $mg \cdot g^{-1}$ at pH=2) and MG (q_e=39.61 $mg \cdot g^{-1}$ at pH=10). The Langmuir and Freundlich isotherm models were applied to explain the adsorption process of dyes on the surface of LDH. The Langmuir model (R^2=0.991 and 0.999 for Eosin Y and Malachite G, respectively) was very appropriate to explain the process of adsorption on NiCoAl-LDH as homogeneous (monolayer). The maximum adsorption capacity of EY and MG calculated with Langmuir model was 78.74 and 110.13 $mg \cdot g^{-1}$ at 30 °C, respectively. Also with 240 minutes contact time 94.8% EY and 89.9% MG was adsorbed by as synthesized NiCoAl-LDH nanosheets. The NiCoAl-LDH nanosheets showed excellent performance of reusability of up to five regeneration cycles. The results showed that the adsorption capacity of NiCoAl-LDH nanosheets after five regeneration cycles, to adsorb EY, decreased only from 40.80 to 36.93 $mg \cdot g^{-1}$ and that of MG from 79.21 to 75.42 $mg \cdot g^{-1}$, which is acceptable. The overall results Suggest that the fabricated NiCoAl-LDH is favorable for the purification of dye contaminated water.

Keywords: LDH, Layered Double Hydroxide, NiCoAl-LDH, Eosin Yellow, Malachite Green, Dye Adsorption, Purification of Water

INTRODUCTION

Sufficient quantity of hygienic and safe drinking water is fundamental to human health [1]. Water pollution has become a much serious and critical issue due to recent development of worldwide industrial and economic activities [2,3]. Many industrial units extensively use various kind of dyes and pigments such as leather tanning, textile, paper, paint, plastic, printing, electroplating, pharmaceutical and cosmetic industries [4]. These harmful dyes, due to their carcinogenic and mutagenic nature, cause various kinds of disorders by affecting lungs, skin, and digestive system [5]. For example, Eosin yellow (EY) with high solubility in water and high usage on commercial scale has many health concerns, like irritation to skin and eyes and damage to lungs, kidneys and liver [6]. Similarly, Malachite green (MG), which has mutagenic and carcinogenic effects on animal as well as human health, is extensively used in many industrial processes [4,7]. Many techniques have been adopted to eliminate these pollutants from water, including photo-degradation [8-10], biological treatment, photo-catalytic oxidation of organic pollutants [11,12] chemical oxidation, membrane technology, adsorption [13,14] and catalysis [15-17].

The adsorption process for the elimination of dyes is considered the best, owing to its high efficiency, simple design, easy operation and effectiveness of processing and production cost [14,18]. Even though, many types of natural adsorbents like tea leaf litter powder [19], pine apple peels [20], pomegranate peels [4] and synthetic adsorbent materials like graphene [21], activated carbon [22], porous carbon [23], modified silica [24], clays [25], polymers [26] and zeolites [27] are widely used for the adsorption of dyes. But these commonly used adsorbents have very low capability to adsorb contaminants from water or they have high production cost. Therefore, more work still is required to discover adsorbents which have high efficiency for the adsorption removal of contaminants (dyes,

†To whom correspondence should be addressed.
E-mail: umair.azhar9922@gmail.com, shoaib03ahmad@outlook.com, azizypk@yahoo.com

heavy metal ions and antibiotics) from polluted water. Consequently, layered double hydroxides (LDH) are preferred for adsorption removal of dyes, owing to extraordinary stability in water, simple synthesis process, low production cost, low toxicity and recyclability [28,29].

LDH are hydrotalcite-like materials having two-dimensional (2D) nanostructure and the chemical composition is generally symbolized as $[M^{2+}(1^{-X})M^{3+}(X)(OH)_2]X+(An^{-})X/n.mH_2O$, where An^{-} represents interlayer anions, while M^{3+} and M^{2+} are trivalent and bivalent metal ions, respectively [30,31]. These 2D materials (LDH) have many built-in characteristics like chemical multifunctionality, replaceable intercalated anions and non-toxicity [32]. LDH have very broad applications in the fields of adsorption [13,33], catalysis [34], CO_2 capturing [35] energy storage [36,37], oxygen reduction reaction [38], and drug delivery [39].

Owing to its unique structure and comparatively simple synthesis approach of LDH, substantial development has been attained in the research and progress of applications for LDH in adsorptive removal of pollutants from aqueous solutions. So far, various simple and hybrid LDH have been produced for adsorption application of heavy metal ions and toxic organic dyes from water. For example, Zubair et al. [40] synthesized NiFe-LDH for the adsorption removal of Eriochrome black T from water. Khodam et al. [41] fabricated NiCoAl-LDH for elimination of Acid red 14 from water. Clark et al. [42] synthesized Zn_2Al-CO_3-LDH to adsorb Reactive orange 16 and Reactive black 5 from water. Guo et al. [43] produced ZnAl-LDH/$Al(OH)_3$ nanosheets to remove Congo red and Methyl orange from water. However, simple LDH alone may not be proved an efficient adsorbent due to its low surface area and porosity. To overcome this problem, hybrid mix LDH with heterogeneous transition metals was produced as an emergent material for the adsorption of toxic dyes from aqueous mediums. These mix hybrid LDH are cost-effective, risk-free, readily available and can easily be restored for recycling [5].

In present work, we produced porous hybrid NiCoAl-LDH, trimetallic layered double hydroxide nanosheets for the concurrent adsorption of reactive dyes like Eosin yellow and Malachite green from water. For comparative study, CoAl-LDH and NiAl-LDH were also fabricated and applied for adsorption of these dyes. The morphology, porosity and crystalline structures of synthesized adsorbents were characterized by various techniques. The adsorption efficiency of these adsorbents was examined at various pH, contact time and concentration of dyes by using kinetic models. It should be highlighted that our synthesized hybrid NiCoAl-LDH nanosheets exhibited excellent adsorption capacity (q_{max}=87.74 $mg{\cdot}g^{-1}$ for Eosin yellow and 110.13 $mg{\cdot}g^{-1}$ for Malachite green) and good recyclability.

EXPERIMENTAL

1. Materials

Nickel nitrate ($Ni(NO_3)_2{\cdot}6H_2O$), cobalt nitrate ($Co(NO_3)_2{\cdot}6H_2O$), 2-methylimidazole, aluminium nitrate ($Al(NO_3)_3{\cdot}9H_2O$), absolute ethanol, methanol, urea, hydrochloric acid, sodium hydroxide, Eosin yellow and Malachite green were purchased from Shanghai Chemical Industrial Company (China). All chemicals, reagents and solvents used were of A grade and no further purification was carried out. For every session of experimentation (synthesis, characterization and application) all relevant solutions were prepared fresh.

2. Synthesis of CoAl-LDH

Following the general synthesis procedure, 5 mmol of aluminium nitrate and 2.5 mmol of cobalt nitrate were dissolved in 400 mL deionized water. After clear solution formation, 17.5 mmol of urea was dissolved in it and the resultant mixture was shifted into a round bottom flask and refluxed at 95 °C for 48 hours. After 48 hours, pinkish color precipitates were formed that were separated by ordinary filtration method, washed several times with hot water and desiccated in convection oven at 75 °C.

3. Synthesis of NiAl-LDH

NiAl-LDH was also prepared with similar method as reported above by replacing cobalt nitrate with nickel nitrate. The reaction mixture was stirred at 95 °C and refluxed for 48 hours. The resultant green precipitates were obtained by filtering the reaction mixture by ordinary filtration method, washed with hot water and de-

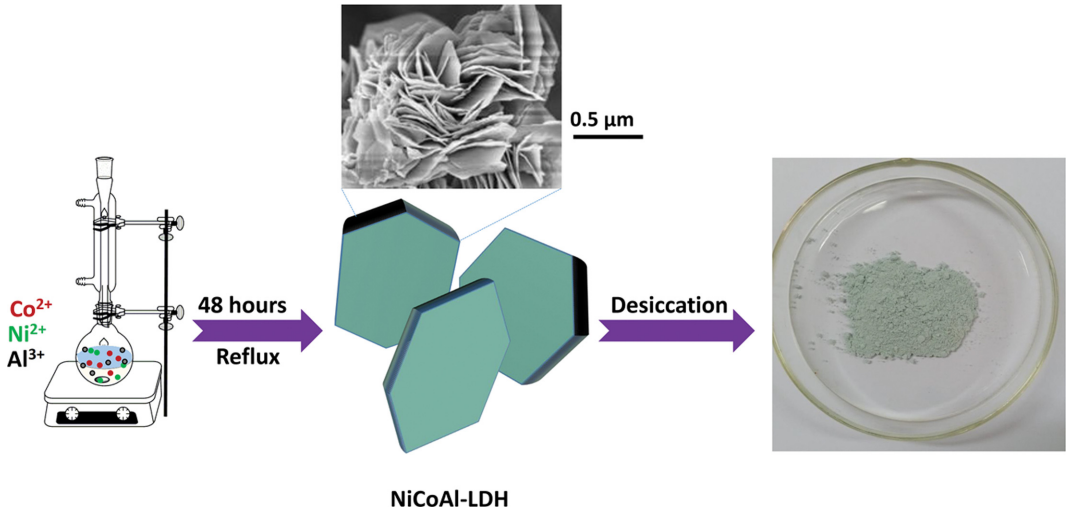

Fig. 1. Schematic representation for the formation of NiCoAl-LDH nanosheets.

siccated in air or oven at 75 °C.

4. Synthesis of Tri-metallic NiCoAl-LDH

Hydrothermal method was used for the fabrication of NiCoAl-LDH (Fig. 1). Typically, $Co(NO_3)_2{\cdot}6H_2O$ (1.25 mmol), $Ni(NO_3)_2{\cdot}6H_2O$ (1.25 mmol), $Al(NO_3)_3{\cdot}9H_2O$ (5 mmol) were dissolved in deionized water, and then 17.5 mmol urea was added and made volume up to 400 mL by adding distilled water. After homogeneous solution formation, it was shifted into a round bottom flask of 500 mL and refluxed at 95 °C for 48 hours. The NiCoAl-LDH precipitates were obtained by filtering the reaction mixture by ordinary filtration method, washed several times with hot water and desiccated in air or oven at 75 °C.

5. Characterization

X-ray diffraction (XRD) patterns of synthesized NiAl-LDH, CoAl-LDH and NiCoAl-LDH nanosheets were taken to identify crystalline phases by using a diffractometer (PANalytical X'Pert powder diffractometer). The morphology of CoAl-LDH, NiAl-LDH and NiCoAl-LDH was examined using scanning electron microscope (SEM, S4500, Hitachi). The TEM images were taken by using high-resolution transmission electron microscopy (HRTEM, JEOL-2100F microscope). The pore size and surface area of synthesized CoAl-LDH, NiAl-LDH and NiCoAl-LDH were analyzed using Micromeritics ASAP 2020 analyzer. UV-Vis spectrophotometer (Shimadzu UV-1240) was used to measure the concentration of dye solution before and after the process of adsorption.

6. Adsorption Experiments of EY and MG

The adsorption kinetic experiments of EY and MG were done by taking 0.01 g adsorbent (CoAl-LDH, NiAl-LDH and NiCoAl-LDH) to adsorb dye from 20 mL solution having dye concentration 20 mg·L^{-1}. The sample mixtures were then shaken at 150 rpm, 30 °C with thermostatic shaker. After a fixed contact time the LDH samples were separated from solution containing remaining dye concentration by centrifuging it at 6,000 rpm for 10 minutes. After that, the concentration of dye solution was measured by using UV-Vis spectrophotometer at wavelength 524 nm and 617 nm; those were the fundamental wavelengths for absorption peak of Eosin yellow and Malachite green, respectively.

The amount of dyes adsorbed (q, mg·g^{-1}) by CoAl-LDH, NiAl-LDH and NiCoAl-LDH nanosheets was calculated by Eq. (1).

$$q = \frac{(C_o - C_e)V}{m} \tag{1}$$

where 'V' symbolizes the dye solution volume in liters and 'm' symbolizes the total mass of adsorbent used. Initial and equilibrium concentration of dye solutions was represented by C_o and C_e (mg L^{-1}), respectively.

The effect of initial pH of dye solution was carried out by measuring adsorption capacity of synthesized adsorbents at pH=2, 6 and 10 by keeping all other parameters like dye concentration, contact time and adsorbent dose constant. Similarly, the effect of contact time was determined by measuring the absorbance of dye solution at time 30, 60, 120, 180 and 240 minutes by keeping all other parameters constant. For adsorption isotherm study, different concentrations (5 to 25 mg L^{-1}) of EY and concentrations (10 to 50 mg L^{-1}) of MG dye solutions were used and the adsorption experiment was carried out by using a spectrophotometer. The EY and MG adsorption capacity of CoAl-LDH, NiAl-LDH and NiCoAl-LDH was calculated by using Eq. (1). The Langmuir (Eq. (2)) [13, 44] and Freundlich (Eq. (3)) [44] isotherm models were applied on the data obtained from spectrophotometer to conduct adsorption study. We agreed to the Langmuir model the adsorption process on the surface of adsorbent done at specific homogeneous sites. No more adsorption process proceeds after the occupation of all available sites present on an adsorbent molecule. This showed that, after monolayer coverage of adsorbent no more adsorption would take place.

$$\frac{C_e}{q_e} = \frac{1}{q_{max}K_L} + \frac{C_e}{q_{max}} \tag{2}$$

where, K_L (L·mg^{-1}) denotes the constant of affinity associated with binding energy of adsorption and adsorbent's maximum adsorption capacity is represented by q_{max} (mg·g^{-1}). q_e (mg·g^{-1}) represents the adsorption capacity of adsorbent at equilibrium.

Freundlich model, presented in Eq. (3), is an empirical equation. The Freundlich isotherm model assumes that the process of adsorption is carried out on various surface layers of the adsorbent, suggested as multilayer adsorption. The Freundlich model can be articulated in the form of equation as

$$\ln q_e = (1/n) \times \ln C_e + \ln K_F \tag{3}$$

In Eq. (3), K_F (mg·g^{-1}) represents constants for adsorption of Freundlich model, and n (g·L^{-1}) denotes the driving force strength of adsorption process. Higher value of 'n' represents the greater feasibility of adsorption to be carried out.

For selection adsorption experiment, a mixture of EY and MG, both having concentration of 20 mg·L^{-1}, was taken and an adsorption experiment was carried out. Individual dye adsorption experiments of EY and MG were also conducted side by side for comparison. For reusability test, the adsorption experiments were done up to five cycles. During each cycle, the same amount of adsorbent and concentration of dye was used in addition to all other variables constant.

RESULTS AND DISCUSSION

1. Characterization

The surface morphology of as-synthesized NiCoAl-LDH was investigated by SEM. The SEM images of NiCoAl-LDH nanosheets preserve repeatedly dispersed shrivel and curly interconnected 2D nanosheets having flower-like microspheres. These nanosheets have several nanometers of thickness and 200-500 nm sideways dimensions (Fig. 2(a)-(b)).

The LDH nanosheets consists of building blocks of interconnected nanoplatelets have open-up network structure formation which is directed by a "heterogeneous nucleation growth" mechanism [37]. The TEM imaging of synthesized NiCoAl-LDH was also executed for further exploration of morphology and structure (Fig. 2(c)-(d)). TEM images reveal that NiCoAl-LDH have ultrathin interconnected nanosheets, which assists the fast diffusion of adsorbed molecules in the process of adsorption [44].

The XRD patterns of fabricated adsorbent samples are presented in Fig. 3. The reflection peaks at 11.7°, 23.5°, 34.8°, 39.2°,

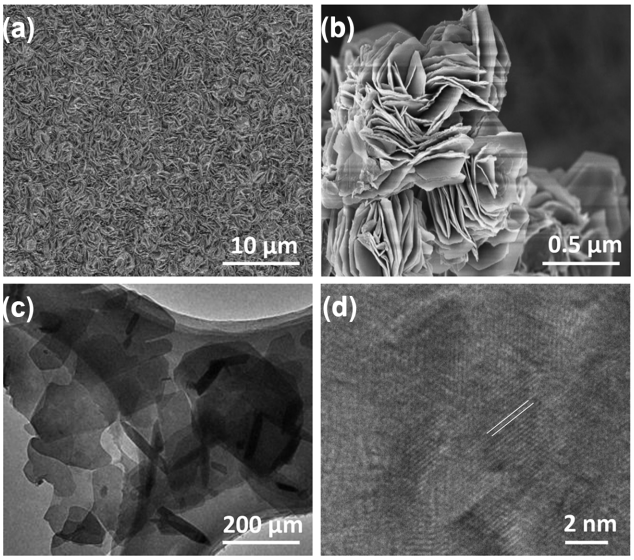

Fig. 2. (a)-(b) SEM images of NiCoAl-LDH, (c)-(d) TEM images of NiCoAl-LDH.

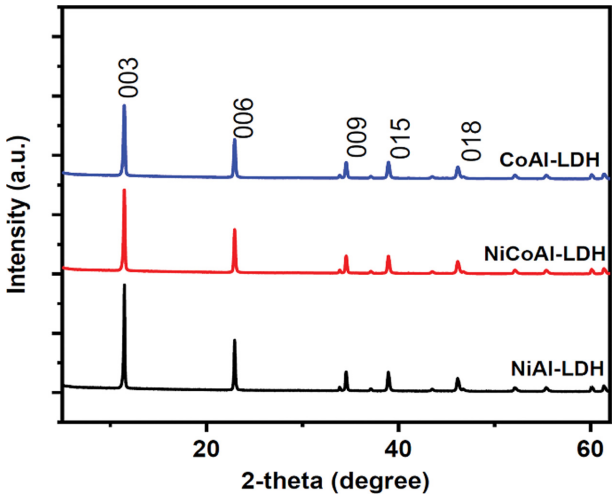

Fig. 3. XRD pattern of CoAl-LDH, NiAl-LDH and NiCoAl-LDH nanosheets.

46.8°, correspond to the [003], [006], [009], [015], [018], reflections of an unsystematically stacked CoAl-LDH phase, respectively [37]. Also, the reflection peaks at 2θ=11.68°, 23.6° and 35.1° correspond to (003), (006) and (009), representing the characteristic reflections of NiAl-LDH [45]. The appearance of the reflection peaks at 11.68°, 23.45°, 31.07°, 34.93°, 39.41°, 47.16° and 60.88° are distinctive of the NiCoAl-LDH [46]. These results demonstrated that the microspheres of NiCoAl-LDH were successfully synthesized by the one-step growth method. It is important to mention here that the diffraction peaks were sharp and symmetric, suggesting high purity and crystallinity in NiCoAl-LDH.

Surface area of adsorbent plays a fundamental role in the process of adsorption. Greater surface area and pore size are the preferred features of adsorbent materials. Due to greater surface area, the adsorbate molecules have greater probability and space to be adsorbed. Also, greater pore size, occupying more dye molecules into it. As shown in Fig. 4(a), the N_2 adsorption isotherms of all three samples of LDH (NiAl-LDH, CoAl-LDH and NiCoAl-LDH) show a Type-IV shape, which suggests that mesopores and macropores are present within these LDH materials [44]. The pore size distribution curves of NiCoAl-LDH sample revealed 2 nm to more than 100 nm broad range of pore size [47].

The adsorbents having mesopores and macropores and high surface area assist the diffusion process of molecules or ions to be adsorbed and thus stimulate adsorption [44]. For NiAl-LDH, CoAl-LDH and NiCoAl-LDH samples, a peak exists between 30 and 33 nm in the pore size distribution curve, which indicates broad mesopore size distribution (Fig. 4(b). The NiCoAl-LDH has a larger surface area (134.21 $m^2 \cdot g^{-1}$) than NiAl-LDH (114.87 $m^2 \cdot g^{-1}$) and CoAl-LDH (109.19 $m^2 \cdot g^{-1}$). The larger specific surface area can assist the distribution of more adsorbed dye molecules due to an increase in the number of active sites, and as a result the adsorption efficiency of adsorbent improved.

2. Effect of PH on Adsorption Capacity

The pH of a dye solution plays an important role in the process of adsorption, as it affects the charge on the surface of adsorbent molecule by altering the chemistry of functional groups attached to adsorbent molecules [48]. Eosin yellow (EY) (Fig. S4), an anionic

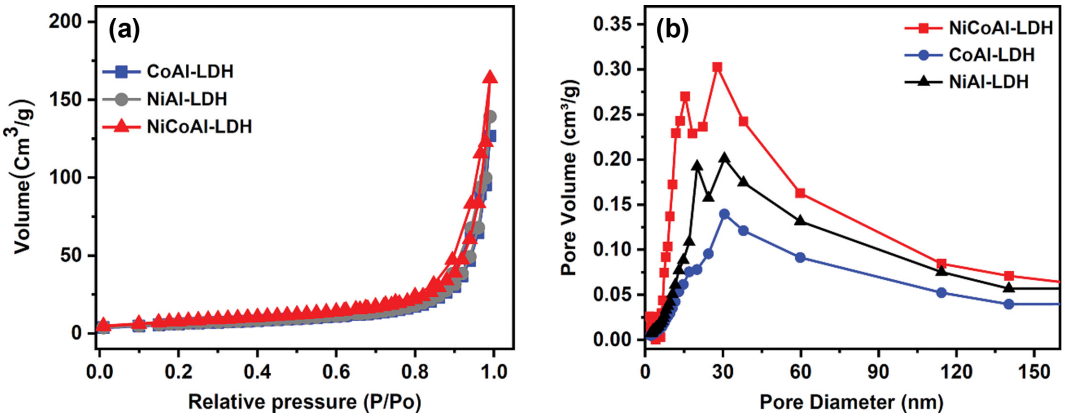

Fig. 4. (a) Adsorption-desorption isotherms and (b) pore size distribution of CoAl-LDH, NiAl-LDH and NiCoAl-LDH nanosheets.

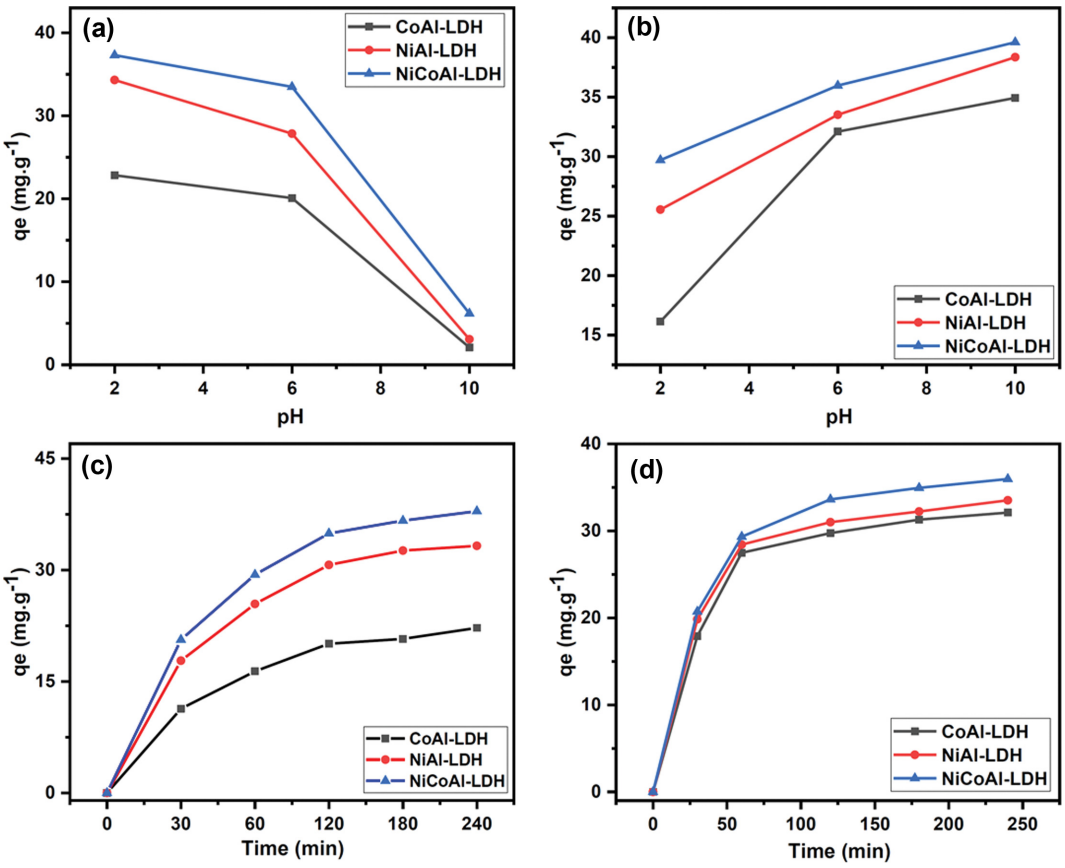

Fig. 5. The adsorption capacities of CoAl-LDH, NiAl-LDH and NiCoAl-LDH at (a) different initial pH of EY, (b) different initial pH of MG, (c) at different contact time with EY, and (d) at different contact time with MG.

dye of the fluorescein class, is extremely soluble in water [6]. Experiments were performed to inspect the effect of pH on the adsorption capability of synthesized adsorbents by keeping all variables like adsorbent dose, contact time with adsorbent, temperature and concentration of dye solution constants, except the pH of dye solution. As shown in Fig. 5(a), it was analyzed that the adsorption of EY dye decreased with the increased pH from 2 to 10. The adsorption capacity (q_e) of our synthesized tri-metallic LDH (NiCoAl-LDH) was 37.30 mg·g^{-1} at pH=2 and 6.17 mg·g^{-1} at pH=10 for EY. Lower adsorption of Eosin yellow dye at higher pH is undoubtedly due to the existence of OH^- ions contending with the anionic functional groups on the dye molecule, and also because of electrostatic repulsion among dye molecules (adsorbate) and adsorbents (CoAl-LDH, NiAl-LDH and NiCoAl-LDH).

But in case of Malachite green the situation is reversed. The adsorption of MG was lower in lower pH (02) and higher in basic pH (10). MG dye is anionic at pH<6.9 and cationic at pH>8 [4]. At pH 10, NiCoAl-LDH showed adsorption (q_e) 39.61 mg·g^{-1} and 29.71 in acidic medium (pH=2), It was analyzed from these results that the MG adsorbed more when the pH of dye solution was alkaline or neutral [49]. Fig. 5(b) shows removal efficiencies of CoAl-LDH, NiAl-LDH and NiCoAl-LDH for MG dye at pH 2.0-10.0. The cations on the surface of LDH might compete with cationic MG, under comparatively higher acidic medium for the active sites of LDH nanosheets, leading to a low removal efficiency. These sites are neutralized in the acidic conditions, which are assumed to be unfavorable events to adsorb cationic dye like malachite green (MG) onto the surface of LDH at the acidic medium. However, when the pH was neutral or alkaline, the electrostatic attractive interaction between positively charges dye (malachite green) and anions present on the surface of adsorbent (LDH) increased, resulting in the increase in the adsorption rate.

3. Effect of Contact Time on Adsorption

The consequence of contact time of adsorbents (CoAl-LDH, NiAl-LDH and NiCoAl-LDH) with dye (Eosin Y and Malachite G) molecules is shown in Fig. 5(c)-(d). It was noticed that the adsorption process of EY and MG onto the surface of LDH (CoAl-LDH, NiAl-LDH and NiCoAl-LDH) was rapid for the first 30 minutes. After that it was trailed off with increasing time of contact. This behavior of adsorbents was due to the fact that, at initial stage all the active sites on adsorbent were vacant and concentration of dye was high. As the time increased the number of active sites decreased due to occupation with dye molecules and rate of adsorption decreased [50]. After the equilibrium was accomplished, no more adsorption could happen due to the possible monolayer of dye formation onto the surface of adsorbent. Due to limited porous behavior of CoAl-LDH, NiAl-LDH and NiCoAl-LDH the time of adsorption is short and equilibrium is attained with less time. After 240 minutes contact time, the CoAl-LDH, NiAl-LDH and NiCoAl-LDH showed equilibrium adsorption capacities of

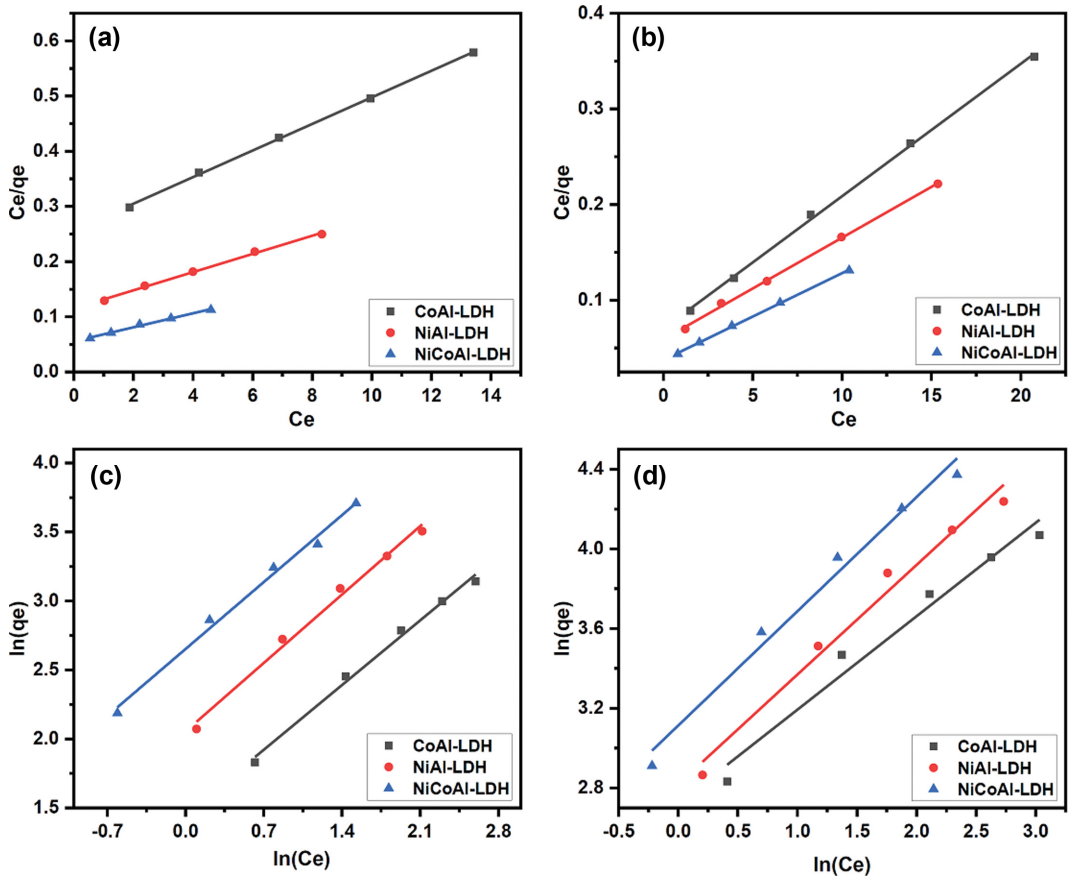

Fig. 6. Langmuir isotherm fittings: (a) for Eosin Y, (b) for Malachite G, (c) Freundlich isotherm fitting results for Eosin Y, and (d) Freundlich isotherm fitting results for Malachite G.

Table 1. The fitting results of Langmuir and Freundlich isotherm models

Dye	Adsorbent	Langmuir model			Freundlich model		
		q_{max} (mg·g^{-1})	K_L (L·mg^{-1})	R^2	K_F (mg·g^{-1})	n (g·L^{-1})	R^2
EY	CoAl-LDH	41.52	0.0938	0.999	4.271	1.492	0.991
	NiAl-LDH	60.67	0.1432	0.996	7.798	1.412	0.988
	NiCoAl-LDH	78.74	0.2284	0.991	14.191	1.443	0.989
MG	CoAl-LDH	72.20	0.1969	0.998	15.23	2.132	0.963
	NiAl-LDH	94.34	0.1794	0.998	16.75	1.8181	0.975
	NiCoAl-LDH	110.13	0.2416	0.999	22.49	1.745	0.976

22.22, 33.26 and 37.92 mg·g^{-1}, respectively, for EY. Similarly, CoAl-LDH, NiAl-LDH and NiCoAl-LDH after 240 minutes contact time showed adsorption capacities of 32.09, 33.51 and 35.96 mg·g^{-1} MG.

4. Adsorption Isotherm Study

To explain the distribution of adsorbate (Eosin yellow and Malachite green) molecules among adsorbents (CoAl-LDH, NiAl-LDH and NiCoAl-LDH) and water at equilibrium, adsorption isotherm studies were carried out. Langmuir and Freundlich models were applied to explain the process of adsorption. Langmuir model suggested that the surface of adsorbent is smooth and homogeneous and adsorption of dye takes place as single layer with equal energy at all active sites [40]. According to Freundlich isotherm model, the surface of adsorbent is not smooth but heterogeneous, and the process of adsorption takes place on multi layers of adsorbate surface [51].

The plots of different parameters of Langmuir and Freundlich models are represented in Fig. 6 and relevant calculated data is represented in Table 1. As depicted in Fig. 6(a)-(b), for all the three LDH (CoAl-LDH, NiAl-LDH and NiCoAl-LDH), the Langmuir model is better fitted than Freundlich model. The R^2 values of the Langmuir isotherm for EY were 0.999, 0.996 and 0.991 of CoAl-LDH, NiAl-LDH and NiCoAl-LDH, respectively, which were greater than R^2 of Freundlich isotherm (CoAl-LDH=0.991, NiAl-LDH=0.988 and NiCoAl-LDH=0.989), indicating the adsorption of EY on the LDH (CoAl-LDH, NiAl-LDH and NiCoAl-LDH) as mono-

layer (Table 1). The q_{max} obtained by Langmuir model was 41.52, 60.67 and 78.20 mg·g^{-1} of CoAl-LDH, NiAl-LDH and NiCoAl-LDH for Eosin Y. Similarly, the high R^2 of the Langmuir isotherm of CoAl-LDH=0.998, NiAl-LDH=0.998 and NiCoAl-LDH=0.999 for MG as compared to (R^2) of Freundlich model (CoAl-LDH=0.963, NiAl-LDH=0.975 and NiCoAl-LDH=0.976) indicated best fitting of Langmuir isotherm model. The q_{max} built on Langmuir model was to be 72.20, 94.34 and 110.13 mg·g^{-1} of CoAl-LDH, NiAl-LDH and NiCoAl-LDH, respectively for MG (Table 1).

The plots of Ce versus qe for both EY and MG were also drawn (Fig. 7). It is clear from Fig. 7 that the NiCoAl-LDH have greater equilibrium capacity than that of NiAl-LDH and CoAl-LDH. Also, the equilibrium adsorption capacity of NiCoAl-LDH is greater towards MG than that of EY at same temperature indicating that NiCoAl-LDH have greater affinity towards MG.

The comparison of adsorption capacity of synthesized NiAl-LDH

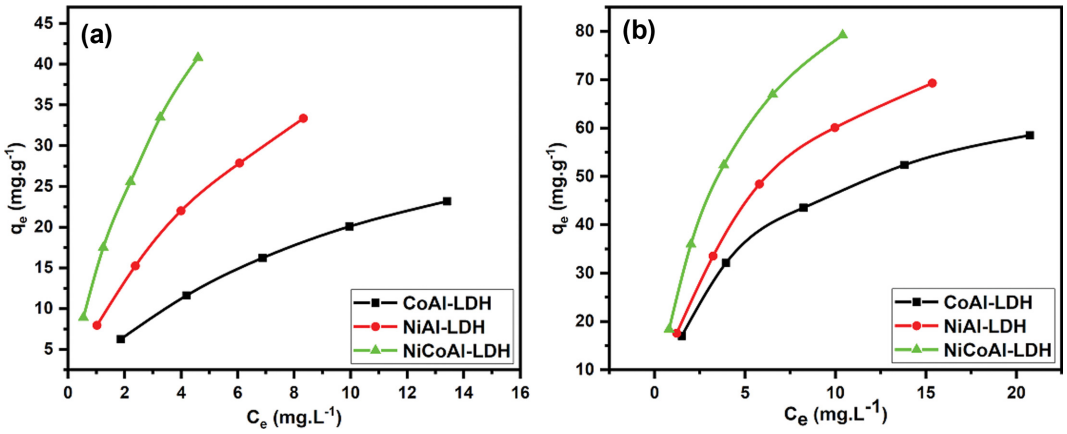

Fig. 7. Equilibrium adsorption capacity q_e versus equilibrium concentrations C_e for the adsorption of dye on CoAl-LDH, NiAl-LDH and NiCoAl-LDH, (a) Eosin yellow, (b) Malachite green.

Table 2. Comparison of adsorption capacity (q_{max}, mg·g^{-1}) of Eosin Yellow (Eosin Y) on different adsorbents

Adsorbent material	q_{max} (mg·g^{-1})	References
Chitosan/PVA	52.91	[52]
Aminosilane-modified cellulose (Cel-SiN)	61.36	[6]
SBE/C	11.15	[25]
Teak leaf litter powder (TLLP)	31.64	[19]
PMAC	40.00	[22]
xGnP® graphite nanoplatelets	66.00	[53]
Sol-gel γ-Al_2O_3 nanoparticles	47.78	[54]
Pineapple peels (PP)	11.76	[20]
CoAl-LDH	41.52	Present study
NiAl-LDH	60.67	Present study
NiCoAl-LDH	78.74	Present study

Table 3. The adsorption capacity (q_{max}, mg·g^{-1}) of adsorbents for malachite green (MG)

Adsorbent material	q_{max} (mg·g^{-1})	References
MIL-53(Al)-NH_2	141.00	[55]
carbonized pomegranate peel (CPP)	31.45	[4]
Alginate/Fe_3O_4	50.00	[56]
Palm flower activated carbon (PFAC)	48.48	[57]
Cellulose	2.42	[58]
Iron humate	19.20	[59]
CNF aerogel	212.70	[60]
Cu-MOFs/Fe_3O_4	113.67	[61]
CoAl-LDH	72.20	Present study
NiAl-LDH	94.34	Present study
NiCoAl-LDH	110.13	Present study

and NiCoAl-LDH nanosheets with other conventional and advanced adsorbents was carried out in Table 2 (for Eosin yellow) and Table 3 (for Malachite green). It can be seen that fabricated NiAl-LDH and NiCoAl-LDH have considerable performance for the adsorption elimination of EY and MG from aqueous mediums.

5. Adsorption Mechanism

The adsorption mechanism of NiCoAl-LDH can be explained with porosity and electrostatic interactions among dye molecules and adsorbent (NiCoAl-LDH). The NiCoAl-LDH has a larger surface area (134.21 $m^2 \cdot g^{-1}$) than NiAl-LDH (114.87 $m^2 \cdot g^{-1}$) and CoAl-LDH (109.19 $m^2 \cdot g^{-1}$). The larger specific surface area can assist the distribution of more adsorbed dye molecules due to increase in number of active sites, and as a result the adsorption efficiency of NiCoAl-LDH improved.

Also, the surface of synthesized NiCo-LDH has positive charge under neutral conditions. Eosin yellow is an anionic dye with high solubility in water. Thus, at lower pH electrostatic attractive interactions exist among dye molecules and NiCoAl-LDH and it can adsorb EY under neutral and acidic environment. Furthermore, NiCoAl-LDH has a strong band at 1,385 cm^{-1} corresponding to the N-O vibration mode of NO_3^- as shown in FT-IR spectra in Fig. S7 (supporting information). However, the peak decreased evidently after adsorption of dye, which specifies that some of the anions between NiCoAl-LDH layers are exchanged by EY. On the other hand, MG is a cationic dye. In basic pH (pH>7) NiCoAl-LDH had negative charge on its outer surfaces in the solution. So MG adsorbed on the surface of it is due to the existence of electrostatic interactions among MG and NiCoAl-LDH. As revealed earlier in Fig. 3(b), the adsorption of MG is high in basic pH. The same adsorption mechanism is proposed for NiAl-LDH and CoAl-LDH. To sum up, NiCoAl-LDH attains the purpose of adsorption of Eosin Y and Malachite G dyes primarily through ion exchange, surface complexation and electrostatic attractive interaction (Fig. 8).

6. Selective Adsorption

An experiment for selectivity in adsorption was carried out by using a mixture of Malachite green and Eosin yellow with equal concentration. The results showed that in the dye mixture, the adsorption efficiency of Malachite green increased from 89.92 to 96.45% with NiCoAl-LDH and that of Eosin yellow decreased from 83.69 to 77.55% (Fig. S9). The increase in adsorption efficiency of MG as compared to EY is because MG is a cationic dye, while EY is an anionic dye [6]. Also, the molecules of Malachite green (molar mass=364.91 g/mol) are smaller in size as compared to Eosin yellow (molar mass=691.84 g/mol). Therefore, due to electrostatic attractive interactions among Malachite green and NiCoAl-LDH, more adsorption was carried out in case of MG and, as a result, the adsorption efficiency increased as compared to Eosin yellow.

7. Reusability

The recyclability of used adsorbent and the synthesis cost are two very important factors for the utilization of adsorbent on commercial scale. To regenerate the used NiCoAl-LDH, an ethanol-washing method was engaged owing to its straightforward operation and cost effectiveness. After adsorption, the adsorbent was washed with ethanol, dried at 70 °C and recycled for another adsorption cycle. The regenerated NiCoAl-LDH was used to adsorb Eosin yellow and Malachite green as shown in Fig. 9. The reusability of NiCoAl-LDH was checked up to five regeneration cycles and adsorption efficiency still remained comparable to that of virgin NiCoAl-LDH. The results showed that the adsorption capacity of NiCoAl-LDH nanosheets after five regeneration cycles, to adsorb EY decreased from 40.80 to 36.93 $mg \cdot g^{-1}$ and that of MG from 79.21 to 75.42 $mg \cdot g^{-1}$. Also, after five regeneration cycles no significant mass loss was observed, which indicated that the synthesized NiCoAl-LDH nanosheets can be reused and proved to be cost effective.

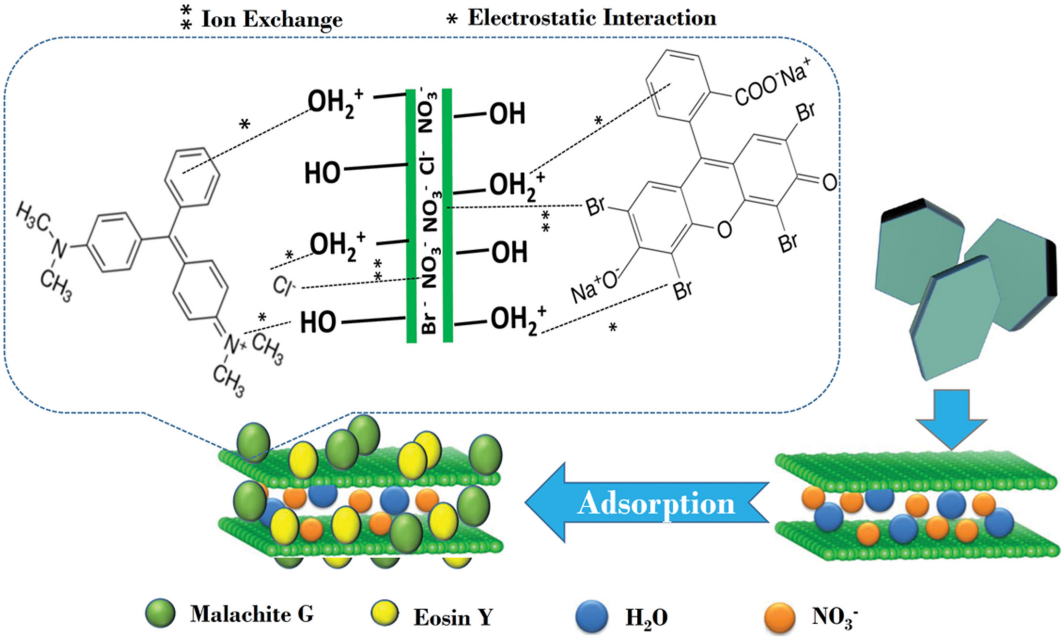

Fig. 8. Proposed adsorption mechanism of EY and MG onto NiCoAl-LDH.

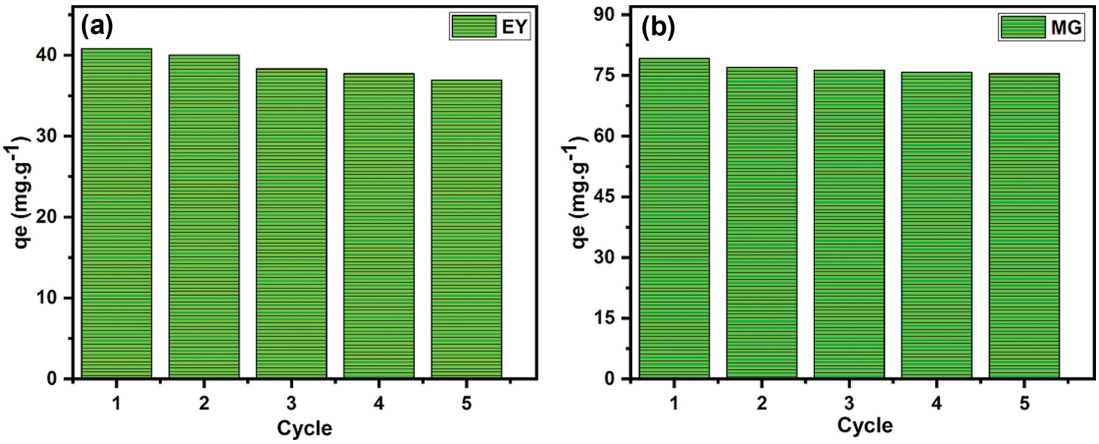

Fig. 9. (a) Efficiency of reused NiCoAl-LDH onto EY up to five regeneration cycles, (b) efficiency of reused NiCoAl-LDH onto MG up to five regeneration cycles.

CONCLUSIONS

Tri-metallic LDH (NiCoAl-LDH) nanosheets were fabricated by urea method and employed for the adsorption removal of Eosin yellow and Malachite green as novel adsorbent. For comparison NiAl-LDH and CoAl-LDH were also fabricated and used for adsorption of dyes. The results revealed that the synthesized NiCoAl-LDH performed best in acidic pH to adsorb EY (q_e=37.30 mg·g^{-1} at pH=2) and in basic pH to adsorb MG (q_e=39.61 mg·g^{-1} at pH=10). Also, with 240 minutes contact time 83.16 and 94.81% of Eosin yellow and 83.79 and 89.92% of Malachite green were adsorbed by NiAl-LDH and NiCoAl-LDH, respectively. The equilibrium adsorption data revealed significant correlation to Langmuir adsorption isotherm: R^2=0.999, 0.996 and 0.991 of CoAl-LDH, NiAl-LDH and NiCoAl-LDH, respectively, for EY and R^2=0.998, 0.998 and 0.999 of CoAl-LDH, NiAl-LDH and NiCoAl-LDH, respectively, for MG indicating good fitting of the Langmuir isotherm. Calculated with Langmuir model, the maximum adsorption capacity of Eosin yellow on as-synthesized NiAl-LDH and NiCoAl-LDH are as higher as 60.67 and 78.74 mg·g^{-1}, respectively, and that of 94.34 and 110.13 mg·g^{-1} of Malachite green on NiAl-LDH and NiCoAl-LDH, respectively. Furthermore, the NiAl-LDH and NiCoAl-LDH nanosheets presented high recyclability. The results disclosed that the adsorption capacity of NiCoAl-LDH nanosheets after five regeneration cycles, to adsorb EY, decreased from 40.80 to 36.93 mg·g^{-1} and that of MG from 79.21 to 75.42 mg·g^{-1}, which is acceptable. The entire study shows that the fabricated NiAl-LDH and NiCoAl-LDH nanosheets with efficient adsorption capability, low cost, high recyclability and minimum/no environmental impact, could be a perfect adsorbent for the prompt elimination of Eosin yellow and Malachite green from water.

DECLARATIONS

List of abbreviations

See Table S1. (Supporting information).

Availability of data and materials

Data and materials will be available on demand.

Competing interests

No competing interests

Funding Information

Deanship of Scientific Research grant number R.G.P. 2/28/42.

AUTHORS' CONTRIBUTIONS

Muhammad Altaf Nazir and Muhammad Aswad Bashir performed the experiments, figured results and wrote the initial draft. Muhammad Imran and Umair Azhar helped to access the spectroscopic instruments, software usage and validation of results. Tayyaba Najam, Muhammad Sohail Bashir and Muhammad Sufyan Javed evaluated the spectroscopic results and formulated the manuscript. Syed Shoaib Ahmad Shah presented idea and developed the protocol. Aziz ur Rehman encouraged Muhammad Altaf Nazir and Muhammad Aswad Bashir to investigate, supervised the findings of this work and revised the manuscript. All authors discussed the results and contributed to the final manuscript.

ACKNOWLEDGEMENTS

The authors would like to acknowledge the Institute of Chemistry, The Islamia University of Bahawalpur, for ensuring facilities for the completion of this project. M. Imran expresses appreciation to the Deanship of Scientific Research at King Khalid University Saudi Arabia through research groups program under grant number R.G.P. 2/28/42.

SUPPORTING INFORMATION

Additional information as noted in the text. This information is available via the Internet at http://www.springer.com/chemistry/journal/11814.

REFERENCES

1. M. A. Nazir, A. Yasar, M. A. Bashir, S. H. Siyal, T. Najam, M. S. Javed,

K. Ahmad, S. Hussain, S. Anjum, E. Hussain S. S. A. Shah and A. u. Rehman, *Int. J. Environ. Anal. Chem.* (2020).
2. H. Lu, L. Zhang, B. Wang, Y. Long, M. Zhang, J. Ma, A. Khan, S. P. Chowdhury, X. Zhou and Y. Ni, *Cellulose.*, **26**(8), 4909 (2019).
3. I. Michael, L. Rizzo, C. McArdell, C. Manaia, C. Merlin, T. Schwartz, C. Dagot and D. Fatta-Kassinos, *Water Res.*, **47**(3), 957 (2013).
4. F. Gündüz and B. Bayrak, *J. Mol. Liq.*, **243**, 790 (2017).
5. M. Daud, A. Hai, F. Banat, M. B. Wazir, M. Habib, G. Bharath and M. A. Al-Harthi, *J. Mol. Liq.*, **288**, 110989 (2019).
6. F. J. L. Ferreira, L. S. Silva, M. S. da Silva, J. A. Osajima, A. B. Meneguin, S. H. Santagneli, H. S. Barud, R. D. S. Bezerra and E. C. Silva-Filho, *Carbohydr. Polym.*, **225**, 115246 (2019).
7. M. A. Nazir, M. A. Bashir, T. Najam, M. S. Javed, S. Suleman, S. Hussain, O. P. Kumar, S. S. A. Shah and A. u. Rehman, *Microchem. J.*, **164**, 105973 (2021).
8. K. Shahzad, T. Najam, M. S. Bashir, M. A. Nazir, A. u. Rehman, M. A. Bashir and S. S. A. Shah, *Inorg. Chem. Commun.*, **123**, 108357 (2021).
9. K. Shahzad, M. Imran Khan, N. Elboughdiri, D. Ghernaout and A. u. Rehman, *Water Environ. Res.*, **93**, 1116 (2021).
10. H. Zhang, W. Guan, L. Zhang, X. Guan and S. Wang, *ACS Omega.*, **5**(29), 18007 (2020).
11. X. Zhao, C. Niu, L. Zhang, H. Guo, X. Wen, C. Liang and G. Zeng, *Chemosphere*, **204**, 11 (2018).
12. M. Jamshaid, A. u. Rehman, O. P. Kumar, S. Iqbal, M. A. Nazir, A. Anum and H. M. Khan, *J. Mater. Sci. Mater. Electron.* (2021).
13. M. A. Nazir, N. A. Khan, C. Cheng, S. S. A. Shah, T. Najam, M. Arshad, A. Sharif, S. Akhtar and A. u. Rehman, *Appl. Clay Sci.*, **190**, 105564 (2020).
14. N. A. Khan, S. Shaheen, T. Najam, S. S. A. Shah, M. S. Javed, M. A. Nazir, E. Hussain, A. Shaheen, S. Hussain and M. Ashfaq, *Toxin Rev.*, (2020).
15. T. Najam, S. Ibraheem, M. A. Nazir, A. Shaheen, A. Waseem, M. S. Javed, S. S. A. Shah and X. Cai, *Int. J. Hydrogen Energy*, **46**(13), 8864 (2021).
16. M. S. Bashir, X. Jiang and X. Z. Kong, *Eur. Polym. J.*, **129**, 109652 (2020).
17. M. S. Bashir, X. Jiang, S. Li and X. Z. Kong, *Front. Chem.*, **7**, 314 (2019).
18. X. Xu, J. Zou, X.-R. Zhao, X.-Y. Jiang, F.-P. Jiao, J.-G. Yu, Q. Liu and J. Teng, *Colloids Surf. A Physicochem. Eng. Asp.*, **570**, 127 (2019).
19. E. O. Oyelude, J. A. Awudza and S. K. Twumasi, *Sci. Rep.*, **7**(1), 1 (2017).
20. F. A. Ugbe, P. O. Anebi and V. A. Ikudayisi, *Int. Ann. Sci.*, **4**(1), 14 (2018).
21. T. Jeyapragasam, *Mater Today: Proceedings.*, **3**(6), 2146 (2016).
22. C. Okey-Onyesolu, C. Okoye and D. Chime, *Int. J. Sci. Eng. Res.*, **9**(3), 140 (2018).
23. L. Borah, M. Goswami and P. Phukan, *J. Environ. Chem. Eng.*, **3**(2), 1018 (2015).
24. H. Zeng, M. Gao, T. Shen and F. Ding, *Colloids Surf. A Physicochem. Eng. Asp.*, **555**, 746 (2018).
25. Y. Liu, Y. Chen, Y. Shi, D. Wan, J. Chen and S. Xiao, *Water Environ. Res.*, **93**, 159 (2021).
26. M. Zhang, Z. Yu and H. Yu, *Polym. Bull.*, **77**(2), 1049 (2020).
27. Z.-L. Cheng, Y.-x. Li and Z. Liu, *Ecotoxicol. Environ. Saf.*, **148**, 585 (2018).
28. S. Ghoreishi and R. Haghighi, *Chem. Eng. J.*, **95**(1-3), 163 (2003).
29. N. Almoisheer, F. Alseroury, R. Kumar, M. Aslam and M. Barakat, *RSC Adv.*, **9**(1), 560 (2019).
30. D. Scarpellini, C. Falconi, P. Gaudio, A. Mattoccia, P. Medaglia, A. Orsini, R. Pizzoferrato and M. Richetta, *Microelectron. Eng.*, **126**, 129 (2014).
31. O. P. Kumar, M. N. Ashiq, S. S. A. Shah, S. Akhtar, M. A. A. Obaidi, I. M. Mujtaba and A. u. Rehman, *Mater. Sci. Semicond. Process.*, **128**, 105748 (2021).
32. M. Sajid and C. Basheer, *Trends Analyt. Chem.*, **75**, 174 (2016).
33. C. Li, M. Wei, D. G. Evans and X. Duan, *Small*, **10**(22), 4469 (2014).
34. C. Cuautli, J. S. Valente, J. Conesa, M. V. n. Ganduglia-Pirovano and J. Ireta, *J. Phys. Chem. C.*, **123**(14), 8777 (2019).
35. D. A. Torres-Rodríguez, E. Lima, J. S. Valente and H. Pfeiffer, *J. Phys. Chem. A.*, **115**(44), 12243 (2011).
36. I. Nicotera, K. Angjeli, L. Coppola, A. Enotiadis, R. Pedicini, A. Carbone and D. Gournis, *Solid State Ion.*, **276**, 40 (2015).
37. J. Han, Y. Dou, J. Zhao, M. Wei, D. G. Evans and X. Duan, *Small*, **9**(1), 98 (2013).
38. T. Najam, S. S. A. Shah, W. Ding, J. Deng and Z. Wei, *J. Power Sources*, **438**, 226919 (2019).
39. L. Li, W. Gu, J. Chen, W. Chen and Z. P. Xu, *Biomaterials*, **35**(10), 3331 (2014).
40. M. Zubair, N. Jarrah, M. S. Manzar, M. Al-Harthi, M. Daud, N. D. Mu'azu and S. A. Haladu, *J. Mol. Liq.*, **230**, 344 (2017).
41. F. Khodam, Z. Rezvani and A. R. Amani-Ghadim, *J. Ind. Eng. Chem.*, **21**, 1286 (2015).
42. I. Clark, J. Smith, R. L. Gomes and E. Lester, *J. Environ. Chem. Eng.*, **7**(3), 103175 (2019).
43. X. Guo, P. Yin and H. Yang, *Micropor. Mesopor. Mater.*, **259**, 123 (2018).
44. H. Hu, J. Liu, Z. Xu, L. Zhang, B. Cheng and W. Ho, *Appl. Surf. Sci.*, **478**, 981 (2019).
45. Y. Sun, J. Zhou, W. Cai, R. Zhao and J. Yuan, *Appl. Surf. Sci.*, **349**, 897 (2015).
46. R. T. Khajeh, S. Aber and M. Zarei, *Renew. Energy*, **154**, 1263 (2020).
47. D. B. Jiang, C. Jing, Y. Yuan, L. Feng, X. Liu, F. Dong, B. Dong and Y. X. Zhang, *J. Colloid Interface Sci.*, **540**, 398 (2019).
48. Richa and A. R. Choudhury, *Carbohydr. Polym.*, **227**, 115291 (2020).
49. K. Gupta and O. P. Khatri, *J. Colloid Interface Sci.*, **501**, 11 (2017).
50. N. Chaukura, E.C. Murimba and W. Gwenzi, *Appl. Water Sci.*, **7**(5), 2175 (2017).
51. M. N. Sepehr, T. J. Al-Musawi, E. Ghahramani, H. Kazemian and M. Zarrabi, *Arab. J. Chem.*, **10**(5), 611 (2017).
52. T. Anita, P. S. Kumar and K. S. Kumar, *J. Water Process. Eng.*, **13**, 127 (2016).
53. E. H. C. d. Oliveira, D. M. d. S. Marques Fraga, M. P. da Silva, T. J. M. Fraga, M. N. Carvalho, E. M. P. de Luna Freire, M. G. Ghislandi and M. A. da Motta Sobrinho, *J. Environ. Chem. Eng.*, **7**(2), 103001 (2019).
54. M. S. Thabet and A. M. Ismaiel, *J. Encapsulation Adsorpt. Sci.*, **6**(03), 70 (2016).
55. C. Li, Z. Xiong, J. Zhang and C. Wu, *J. Chem. Eng. Data*, **60**(11), 3414 (2015).

56. A. Mohammadi, H. Daemi and M. Barikani, *Int. J. Biol. Macromol.*, **69**, 447 (2014).
57. S. Nethaji, A. Sivasamy, G. Thennarasu and S. Saravanan, *J. Hazard. Mater.*, **181**(1), 271 (2010).
58. C. Pradeep Sekhar, S. Kalidhasan, V. Rajesh and N. Rajesh, *Chemosphere*, **77**(6), 842 (2009).
59. P. Janoš, *Environ. Sci. Technol.*, **37**(24), 5792 (2003).
60. F. Jiang, D. M. Dinh and Y.-L. Hsieh, *Carbohydr. Polym.*, **173**, 286 (2017).
61. Z. Shi, C. Xu, H. Guan, L. Li, L. Fan, Y. Wang, L. Liu, Q. Meng and R. Zhang, *Colloids Surf. A Physicochem. Eng. Asp.*, **539**, 382 (2018).

Supporting Information

Kinetics, isothermal and mechanistic insight into the adsorption of eosin yellow and malachite green from water via tri-metallic layered double hydroxide nanosheets

Muhammad Altaf Nazir[*], Tayyaba Najam[**], Muhammad Sohail Bashir[***], Muhammad Sufyan Javed[****], Muhammad Aswad Bashir[*], Muhammad Imran[*****], Umair Azhar[****,†], Syed Shoaib Ahmad Shah[*,***,†], and Aziz ur Rehman[*,†]**

*Institute of Chemistry, The Islamia University of Bahawalpur, Bahawalpur 63100, I. R. Pakistan
**Institute for Advanced Study, Shenzhen University, Shenzhen 518060, P. R. China
***Hefei National Laboratory for Physical Sciences at the Microscale, CAS Key Laboratory of Soft Matter Chemistry, School of Chemistry and Materials Science, University of Science and Technology of China, Hefei, Anhui 230026, P. R. China
****School of Physical Science and Technology, Lanzhou University, Lanzhou 730000, P. R. China
*****Department of Chemistry, Faculty of Science, King Khalid University, P.O. Box 9004, Abha 61413, Saudi Arabia
******Department of Polymer Engineering, National Textile University Karachi Campus, Karachi 74900, I. R. Pakistan
(*Received 27 February 2021 • Revised 27 May 2021 • Accepted 4 July 2021*)

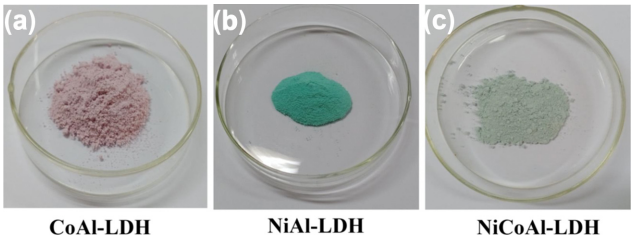

Fig. S1. Synthesized CoAl-LDH, NiAl-LDH and NiCoAl-LDH.

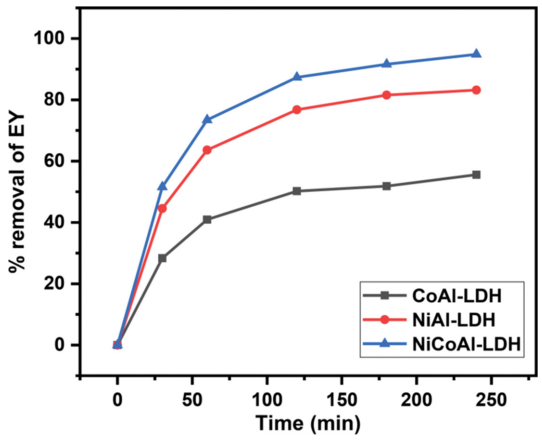

Fig. S2. % removal efficiency of Eosin Y on NiAl-LDH, CoAl-LDH and NiCoAl-LDH.

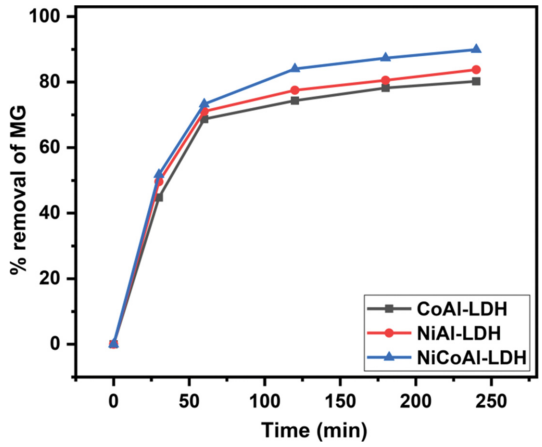

Fig. S3. % removal efficiency of Malachite G on NiAl-LDH, CoAl-LDH and NiCoAl-LDH.

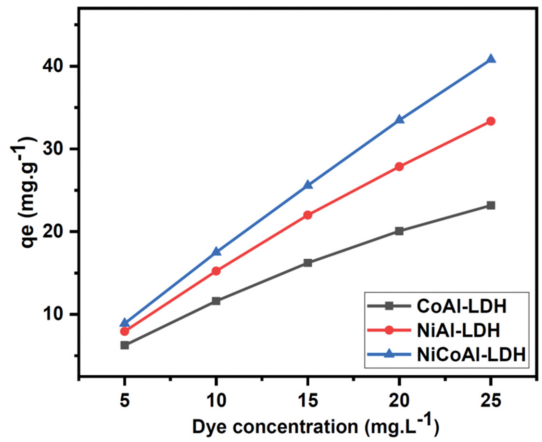

Fig. S4. Adsorption capacity of Eosin yellow on NiAl-LDH, CoAl-LDH and NICoAl-LDH at different initial concentration of dye.

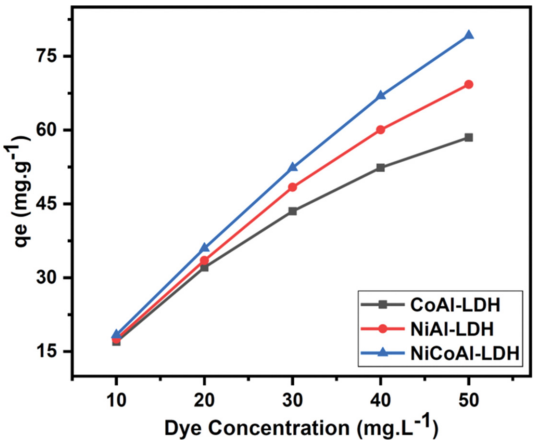

Fig. S5. Adsorption capacity of Malachite green on NiAl-LDH, CoAl-LDH and NICoAl-LDH at different initial concentration of dye.

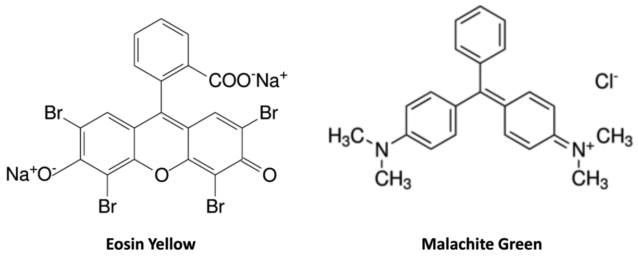

Fig. S6. Structural representation of Eosin yellow and Malachite green.

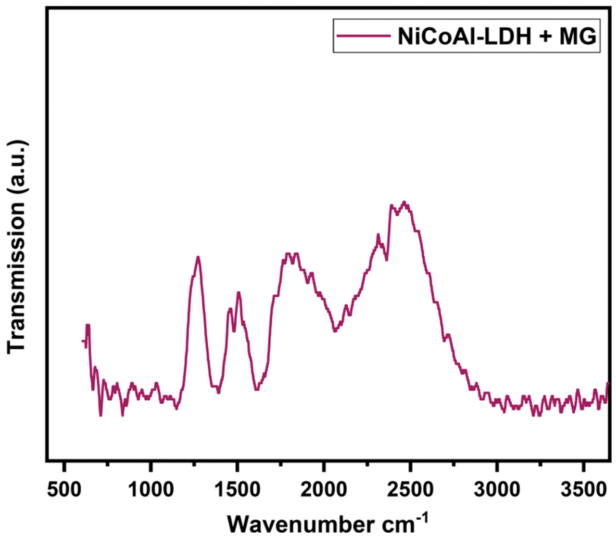

Fig. S7. FT-IR spectra of NiCoAl-LDH after adsorption of Eosin yellow.

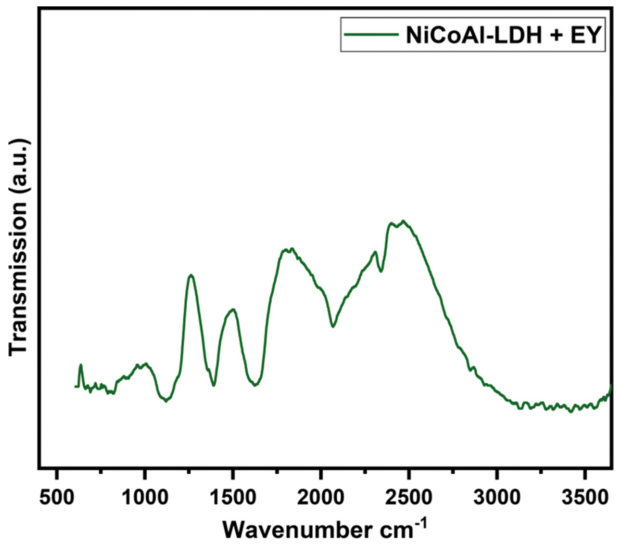

Fig. S8. FT-IR spectra of NiCoAl-LDH after adsorption of Malachite green.

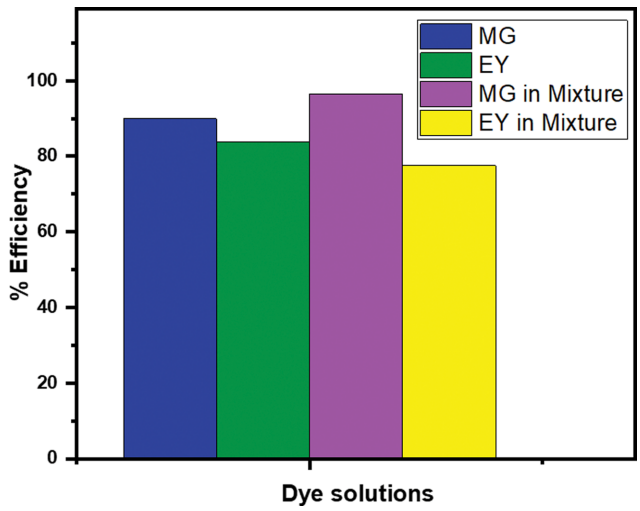

Fig. S9. % age adsorption efficiency of dyes in individual and in mixture of dyes.

Table S1. List of abbreviations

Sr. No.	Abbreviation	Full name
1	SBE/C	Spent bleaching earth based clay/carbon
2	PMAC	Pentaclethra macrophylla based activated carbon
3	PVA	Polyvinyl alcohol
4	EY	Eosin yellow
5	MG	Malachite green
6	LDH	Layered double hydroxide
7	TLLP	Teak leaf litter powder
8	PP	Pineapple peels
8	CPP	Carbonized pomegranate peel
10	PFAC	Palm flower activated carbon